







## Article

# Kaolin Application Modulates Grapevine Photochemistry and Defence Responses in Distinct Mediterranean-Type Climate Vineyards

Sara Bernardo <sup>1</sup>, Ana Luzio <sup>1</sup>, Nelson Machado <sup>2</sup>, Helena Ferreira <sup>1</sup>, Vicente Vives-Peris <sup>3</sup>, Aureliano C. Malheiro <sup>1</sup>, Carlos Correia <sup>1</sup>, Aurelio Gómez-Cadenas <sup>3</sup>, José Moutinho-Pereira <sup>1</sup> and Lia-Tânia Dinis <sup>1,\*</sup>

<sup>1</sup> Centre for the Research and Technology of Agro-Environmental and Biological Sciences (CITAB), University of Trás-os-Montes e Alto Douro, Apt. 1013, 5001-801 Vila Real, Portugal; sbernardo@utad.pt (S.B.); aluzio@utad.pt (A.L.); helenaf@utad.pt (H.F.); amalheir@utad.pt (A.C.M.); ccorreia@utad.pt (C.C.); moutinho@utad.pt (J.M.-P.)

<sup>2</sup> CoLAB Vines&Wines-National Collaborative Laboratory for the Portuguese Wine Sector, Associação Para o Desenvolvimento da Viticultura Duriense (ADVID), Régia Douro Park, 5000-033 Vila Real, Portugal; nelson.machado@advid.pt

<sup>3</sup> Department de Ciències Agràries i del Medi Natural, Universitat Jaume I, E-12071 Castellón de la Plana, Spain; tico\_vives@hotmail.com (V.V.-P.); aurelio.gomez@uji.es (A.G.-C.)

\* Correspondence: liatdinis@utad.com



**Citation:** Bernardo, S.; Luzio, A.; Machado, N.; Ferreira, H.; Vives-Peris, V.; Malheiro, A.C.; Correia, C.; Gómez-Cadenas, A.; Moutinho-Pereira, J.; Dinis, L.-T. Kaolin Application Modulates Grapevine Photochemistry and Defence Responses in Distinct Mediterranean-Type Climate Vineyards. *Agronomy* **2021**, *11*, 477. <https://doi.org/10.3390/agronomy11030477>

Academic Editor: Fabio Fiorani

Received: 2 February 2021

Accepted: 28 February 2021

Published: 4 March 2021

**Publisher's Note:** MDPI stays neutral with regard to jurisdictional claims in published maps and institutional affiliations.



**Copyright:** © 2021 by the authors. Licensee MDPI, Basel, Switzerland. This article is an open access article distributed under the terms and conditions of the Creative Commons Attribution (CC BY) license (<https://creativecommons.org/licenses/by/4.0/>).

**Abstract:** At a local scale, kaolin particle-film technology is considered a short-term adaptation strategy to mitigate the adverse effects of global warming on viticulture. This study aims to evaluate kaolin application effects on photochemistry and related defence responses of *Touriga Franca* (TF) and *Touriga Nacional* (TN) grapevines planted at two Portuguese winegrowing regions (Douro and Alentejo) over two summer seasons (2017 and 2018). For this purpose, chlorophyll *a* fluorescence transient analysis, leaf temperature, foliar metabolites, and the expression of genes related to heat stress (*VvHSP70*) and stress tolerance (*VvWRKY18*) were analysed. Kaolin application had an inhibitory effect on *VvHSP70* expression, reinforcing its protective role against heat stress. However, *VvWRKY18* gene expression and foliar metabolites accumulation revealed lower gene expression in TN-treated leaves and higher in TF at Alentejo, while lipid peroxidation levels decreased in both treated varieties and regions. The positive kaolin effect on the performance index parameter (PI<sub>ABS</sub>) increased at ripening, mainly in TN, suggesting that stress responses can differ among varieties, depending on the initial acclimation to kaolin treatment. Moreover, changes on chlorophyll fluorescence transient analysis were more pronounced at the Douro site in 2017, indicating higher stress severity and impacts at this site, which boosted kaolin efficiency in alleviating summer stress. Under applied contexts, kaolin application can be considered a promising practice to minimise summer stress impacts in grapevines grown in Mediterranean-like climate regions.

**Keywords:** foliar spray; heat stress; high light; JIP-test; particle-film; resilience

## 1. Introduction

In the last decades, the Mediterranean-like climate regions were mostly classified as climate change hotspots, where the impacts of climate variability are likely to change the well-known conceptual factors (i.e., social, cultural, environmental, and economic) of the viticultural sector in the upcoming years [1,2]. Along with the foreseen occurrence of extreme weather events, the combined incidences of several environmental stresses over the summer season (e.g., high irradiance, temperature, and drought) in Mediterranean-type climate areas have also been related to impaired photochemistry and cell homeostasis, limiting both growth and crop yield [3]. Simultaneously, climate variability promotes

several physiological and cellular responses, enabling plants to acclimate under climatic uplines [2,4].

It is well known that environmental stresses, particularly heat stress, induce gene expression and synthesis of heat-shock proteins (HSP), known by their functions as chaperones for newly synthesised proteins, protecting plant cell from damage [5]. In addition, abiotic stresses can also change the expression pattern of a large family of genes (*WRKY* family) that is involved in drought, heat, and salinity tolerance mechanisms, as well as on the regulation of plant development, seed dormancy and germination, leaf senescence, and hormonal signalling [6]. Moreover, the accumulation of osmolytes, like proline and antioxidant compounds (e.g., ascorbate), is a typical plant response to stress exposure [7,8]. Although most research on plant stress responses has been carried out in young plants and under controlled conditions [4,9], there is still little scientific understanding when transposing that knowledge to adult plants under field and commercial conditions.

Scientific outcomes regarding particle film application in grapevines reported a generally positive effect on plant photosynthetic performance, leaf cooling, leaf water status, hormonal balance, and sugar transport, decreasing lipid peroxidation and proline accumulation [10–14]. However, it is still unclear whether kaolin (K) particle film efficiency can be varietal dependent in its interactions with climate variability over consecutive years. In this sense, this study examines kaolin application effects on *Touriga Franca* (TF) and *Touriga Nacional* (TN) grapevine varieties over two consecutive growing seasons, located in distinct Portuguese wine growing-regions (Douro and Alentejo) through a multi-level approach (physiological, biochemical, and molecular). By assessing *VvHSP70* and *VvWRKY18* gene expression, accumulation of stress-related foliar metabolites, and photochemistry responses and performance by transient chlorophyll *a* fluorescence analysis using the JIP-test, this study aims to uncover kaolin foliar coating effectiveness in adult field-grown grapevines in two successive summer seasons.

## 2. Materials and Methods

### 2.1. Site Description

The experiments were carried out over the 2017 and 2018 growing seasons, at two commercial vineyards located in two distinct winegrowing regions: Douro demarcated region (“*Quinta do Orgal*” commercial vineyard: 41°04′ N, 7°04′ W, 169 m), in the northeast of Portugal, hereafter designated as Douro; and Alentejo demarcated region (“*Herdade do Esporão*”, 38°23′ N, 7°33′ O, 220 m), in the southeast part of the country, hereafter referred to as Alentejo. The Alentejo trial displays a slight slope (5° N) and N–S orientation, composed by 8-year-old vines grafted onto 1103P rootstock and trained to bilateral cordon, while the Douro vineyard is installed on a steep slope (30° N) with E–W orientation, composed by 6-year-old vines grafted onto 110R rootstock, and trained to unilateral cordon. Both vineyards present 2.2 × 1.0 m spacing between vines. According to the world reference base for soil resources [15], the soil mapping of both regions is classified as Luvisols, characterised by a clay-enriched subsoil.

### 2.2. Plant Material, Treatments, and Sampling

In both locations, two *Vitis vinifera* L. red varieties were selected, *Touriga Franca* (TF) and *Touriga Nacional* (TN), due to their ability to ripen under intense heat and relevance for the potential quality and typicity of regional Portuguese red wines. The experimental setup was adapted to the existing characteristics of each vineyard to ensure similar edaphoclimatic conditions and sun exposure among treatments and varieties. At Douro, 60 vines per variety were selected, divided into three rows with 20 vines each, while at ‘Alentejo’, we selected 120 vines per variety planted in one extended row, and considered half row as the control group, and the other half as the treated group. In each half row, vines were distributed in three blocks with 20 plants each. Vines were managed according to the growers’ commercial organic practices and deficit irrigated (30% of the reference evapotranspiration) to prevent plant death. In both sites, plants were split into

two experimental groups: the control or untreated group of each variety (TF\_C and TN\_C), and the kaolin treated group (TF\_K and TN\_K). Treated vines were sprayed with kaolin (Surround<sup>®</sup> WP, Engelhard Corporation, Iselin, NJ, USA), prepared in an aqueous solution at the manufacturer recommended dosage of 5% (*w/v*), supplemented with 0.1% (*v/v*) Tween<sup>®</sup> 20 (Sigma-Aldrich, St. Louis, MO, USA, CAS number 9005-64-5) to improve adherence, which was directly applied to leaves according to standard operating procedures adjusted for agricultural practices. In 2017 and 2018, kaolin was applied at the Douro experiment in the windless mornings of 26 June (day-of-year (DOY) 177) and 24 July (DOY 205), respectively. At the Alentejo vineyard, kaolin was applied on July 17 (DOY 198) in both growing seasons. The adjacent control plants were carefully protected by a plastic film during the kaolin application. For all the physiological measurements, 18 healthy, fully expanded, and mature leaves, in a similar position, were sampled per treatment at midday in each sampling date. The measurements were also undertaken at two different developmental stages, according to the Coombe [16] classification: EL35, corresponding to *veraison* (DOY 199 and DOY 212 at Douro, and DOY 208 and DOY 209 at Alentejo in 2017 and 2018, respectively), and EL38, corresponding to the ripening stage (DOY 234 and DOY 254 at Douro, and DOY 237 and DOY 243 at Alentejo in 2017 and 2018, respectively). For all biochemical and molecular assays, leaves were immediately frozen in liquid nitrogen and stored at  $-80\text{ }^{\circ}\text{C}$  for further analyses.

### 2.3. Weather Conditions and Characterisation of the Study Areas

The regions are characterised by a warm-temperate climate with dry and hot summers [17], and rainfall concentrated during the winter months. Based on the Multicriteria Climatic Classification System (MCC System), three bioclimatic indices were chosen [18]: (i) the Huglin Heliothermal Index (HI), which includes mean and maximum temperatures and a day-length factor for a proxy for radiation; (ii) the Cool Night Index (CI), a strictly thermal index, which accounts for mean minimum temperature during maturation (September in the northern hemisphere); (iii) and the Dryness Index (DI), consisting of an adaptation of the potential soil water balance. Regarding thermal conditions, the HI indicated a very warm viticultural climate structure during the experiments (Table 1), excepting the 2018 growing season in Alentejo, which was classified as warm. Complementary to HI and thermal regime, the CI indicated that night temperature conditions in both regions were mostly considered as temperate. Related to the level of potential soil water availability, the DI was mostly rated as very dry in both regions under study. An automatic weather station was set up in each trial site, recording standard meteorological variables, such as the minimum and maximum air temperatures, and precipitation (Figure 1). The occurrence of heatwave events was also assessed by sorting at least five consecutive days with maximum air temperature above  $40\text{ }^{\circ}\text{C}$  [19]. In the Douro experiment, two heatwaves were recorded in 2017 (DOY 165–169 and DOY 193–198), and one in 2018 (DOY 213–218). Similarly, two heatwave events were also recorded at the Alentejo site in 2017 (DOY 167–171 and DOY 192–197), and one in the 2018 growing season (DOY 213–218). In 2017, total precipitation at the Douro and Alentejo regions during the experiments was 65.0 and 31.6 mm, respectively, whereas in 2018, total precipitation of 173.8 and 80.4 mm was recorded in the Douro and Alentejo sites, respectively.

**Table 1.** Huglin Heliothermal Index (HI), Cool Night Index (CI,  $^{\circ}\text{C}$ ), and Dryness Index (DI, mm) values for 2017 and 2018 growing seasons in the Douro and Alentejo sites were considered according to Tonietto and Carbonneau [18].

| Region   | Season | HI   | Class     | CI   | Class            | DI     | Class          |
|----------|--------|------|-----------|------|------------------|--------|----------------|
| Douro    | 2017   | 3283 | Very warm | 14.2 | Temperate nights | −147.1 | Very dry       |
|          | 2018   | 3022 | Very warm | 16.5 | Temperate nights | −47.0  | Moderately dry |
| Alentejo | 2017   | 3148 | Very warm | 13.5 | Cool nights      | −207.6 | Very dry       |
|          | 2018   | 2887 | Warm      | 16.4 | Temperate nights | −119.5 | Very dry       |

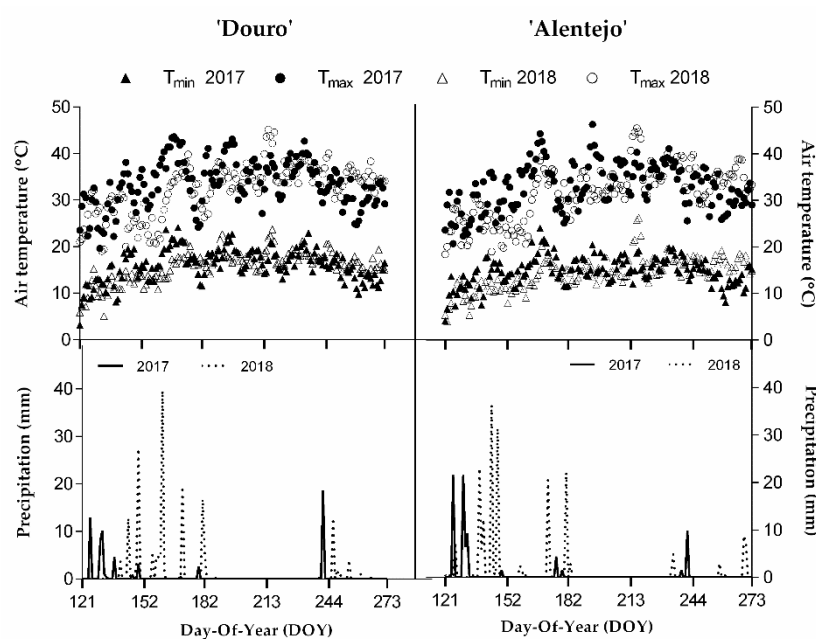


**Figure 1.** Daily minimum and maximum air temperature ( $^{\circ}\text{C}$ ), and precipitation (mm) of 2017 and 2018 growing seasons at both Douro and Alentejo sites.

#### 2.4. Gene Expression by RT-qPCR

RNA was extracted from frozen leaves (0.1 g in triplicates) previously grounded in a fine powder, following the rapid-cetyltrimethylammonium bromide (CTAB) method of Gambino et al. [20] in both EL35 and EL38 stages of 2017 and 2018 growing seasons. Afterwards, RNA samples were treated with DNase I RNase-free (Thermo Scientific, Waltham, MA, USA) to degrade the possible extracted DNA following the manufacturer instructions. The RNA concentration was estimated using the absorbance values at 260 nm with a NanoDrop 2000 spectrophotometer (Thermo Scientific, Waltham, MA, USA), while the purity of each sample was determined calculating the 260/280 and 260/230 ratios. Finally, total RNA (1  $\mu\text{g}$ ) was reverse transcribed to cDNA using PrimeScript RT Reagent Kit (Takara, Shiga, Japan). Quantitative real-time PCR (RT-qPCR) was conducted with an ABI Step One detection system (Applied Biosystems, Foster City, CA, USA). Gene specific primer pairs used for each target or reference gene are listed on Appendix A (Table A1).

The amplification was performed in a reaction containing 1  $\mu\text{L}$  of cDNA, 5  $\mu\text{L}$  of Maxima SYBR Green/ROX qPCR mix (Thermo Scientific), 1  $\mu\text{L}$  of primers (a mix of forward and reverse, 10  $\mu\text{M}$ ), and 3  $\mu\text{L}$  of sterile deionised water. RT-qPCR reactions included a pre-incubation at 95  $^{\circ}\text{C}$  for 10 min, followed by 40 cycles of denaturation at 95  $^{\circ}\text{C}$  for 10 s, annealing at 60  $^{\circ}\text{C}$  for 10 s, and extension at 72  $^{\circ}\text{C}$  for 20 s. Actin (*VvACT2*) and tubulin (*VvTUB2*) were used as housekeeping genes to normalise the results among samples. Relative expression of *VvHSP70* (Phytozome accession no. GSVIVT01008331001), and *VvWRKY18* (Phytozome accession no. GSVIVT01035885001) was achieved using the Relative Expression Software Tool Solver v.2 (REST-MCS) [21,22]. For each analysed gene, they were considered significantly upregulated and downregulated in the kaolin treated groups (TN\_KL and TF\_KL) when their relative expression fold change was  $\geq 2.0$  and  $\leq 0.5$ , respectively.

#### 2.5. Leaf Temperature and Chlorophyll Measurements

In 2017 and 2018 growing seasons, leaf temperature was measured with an infrared thermometer (Infratrace KM800S, Welwyn Garden City, Hertfordshire, UK) with a 15 $^{\circ}$  field view at stages EL35 and EL38, during the midday period. Measurements were performed on sun-exposed and fully expanded leaves at the middle of the shoots. The average temperature of 30 randomly selected leaves of each experimental groups was obtained

by holding the thermometer approximately 1 m above the foliar surface. Chlorophyll concentration per area was estimated using a Chlorophyll Content Meter—CCM-300 (Opti-Sciences, Hudson, NH, USA) at the midday period in the same 30 leaves used for the leaf temperature measurements at both developmental stages under study. Measurements were determined by the average of three readings in distinct parts of the sun-exposed leaf surface.

#### 2.6. Determination of Foliar Metabolites

The lipid peroxidation products were quantified according to Hodges et al. [23]. The extraction was performed by adding 3.0 mL of 20% (*w/v*) trichloroacetic acid, with measurements of the supernatant at 440, 532, and 600 nm in a microplate multiscan reader (SPECTROstar Nano, BMG Labtech GmbH, Offenburg, Germany). After subtracting the non-specific absorbance at 600 nm, the thiobarbituric acid reactive substances (TBARS) were calculated using the malondialdehyde (MDA) extinction coefficient of  $157 \text{ mM cm}^{-1}$ . Lipid peroxidation was expressed in mmol MDA equivalents  $\text{g}^{-1}$  dry weight (DW). Free proline content was extracted with 3% (*w/v*) sulfosalicylic acid (SSA), and centrifuged at 4000 rpm for 15 min at 4 °C as described by Bates et al. [24]. In a test tube (2.0 mL), the reaction mixture containing 250  $\mu\text{L}$  extract, 250  $\mu\text{L}$  acid ninhydrin, and 250  $\mu\text{L}$  glacial acetic acid was incubated in a boiling water bath for 1 h. Then, 500  $\mu\text{L}$  of toluene was added and mixed for 20 s. The upper reddish-pink coloured phase was separated, and absorbance was read at 520 nm in a microplate reader. The colorimetric response was compared to a standard curve based on commercial proline, and results were expressed as  $\mu\text{mol g}^{-1}$  of DW. Ascorbic (AsA) and dehydroascorbic (DAsA) acids were determined following the method of Okamura [25] with slight modifications. Briefly, 10 mg of leaf sample were homogenised in 3.0 mL 6% TCA, and centrifuged for 30 min at 4000 rpm and 4 °C. Then, 100  $\mu\text{L}$  of extract, 100  $\mu\text{L}$  of 150mM- $\text{NaH}_2\text{PO}_4$  buffer (pH 7.4), and 50  $\mu\text{L}$  of 10mM dithiothreitol (DTT) were added to test tubes (2.0 mL), mixed vigorously in a vortex, and incubated 15 min on ice to reduce the DAsA present in the extract. To remove excess DTT, 50  $\mu\text{L}$  of 0.5% (*w/v*) N-ethylmaleimide were added. The samples were then mixed and incubated for 5 min at 25 °C. For the quantification of AsA, water was added instead of DTT, being the volume of both samples equal. To both samples, the following reagents were added consecutively: 200  $\mu\text{L}$  of 10% (*w/v*) TCA, 200  $\mu\text{L}$  of 44% (*v/v*) phosphoric acid, 200  $\mu\text{L}$  of 4% (*w/v*) 2,2'-dipyridyl in 70% ethanol, and 100  $\mu\text{L}$  of 3% (*w/v*)  $\text{FeCl}_3$ . After mixing, the samples were incubated 1 h at 37 °C, and absorbance was recorded at 525 nm. The concentration of DAsA was estimated by subtracting the AsA concentration measured from the total ascorbate quantified. Calibration was done using a standard curve prepared with L-ascorbic acid (Sigma) in 6% TCA, and results were expressed in  $\text{mg g}^{-1}$  of dry weight (DW).

#### 2.7. Chlorophyll *a* Fluorescence Measurements

Chlorophyll *a* fluorescence measurements were carried out in both growing seasons (2017 and 2018), at EL35 and EL38 stages, during the midday period, in six fully expanded and sun exposed leaves per treatment, using a portable chlorophyll fluorimeter OS-30p (Opti-Sciences Inc., Hudson, NH, USA). The leaves were dark-adapted with clips for 30 min before chlorophyll *a* fluorescence transient measurements. The transients were induced by 1 s illumination providing a maximum light intensity of  $3000 \mu\text{mol (photon) m}^{-2} \text{ s}^{-1}$ . The fast fluorescence kinetics ( $F_0$  to  $F_m$ ) was recorded from 10  $\mu\text{s}$  to 1 s. The fluorescence intensity at 50  $\mu\text{s}$  was considered as  $F_0$  [26].

#### 2.8. Analysis of Fluorescence Transients Using JIP Test Parameters

The relative change of the JIP test variables in the Douro and Alentejo regions, for both growing seasons, regards to the midday period of each developmental stage (EL35 and EL38), since is considered a critical period of extreme atmospheric demand conditions. The biophysical parameters derived from the OJIP transient were calculated according to

the JIP test equations [27,28], providing structural and functional information regarding photosystem II (PSII). The following parameters were used: (1) specific energy fluxes per reaction centre (RC)–absorption ( $ABS/RC$ ); electron transport ( $ET_0/RC$ ); trapping ( $TR_0/RC$ ), and dissipation ( $DI_0/RC$ ); (2) phenomenological energy fluxes per excited cross-section (CS)–absorption ( $ABS/CS$ ); (3) flux ratios or yields–maximum quantum yield of primary photochemistry ( $\Phi P_0$ ), electron transport probability ( $\Psi_0$ ), and the quantum yield of electron transport ( $\Psi E_0$ ); (4) performance index ( $PI_{ABS}$ ) on an absorption basis, measuring the performance up to the photosystem I (PSI) end electron acceptors.

### 2.9. Statistical Analysis

Statistical analyses of leaf temperature, chlorophyll content, foliar metabolites, and chlorophyll *a* fluorescence transients were performed using Sigma-Plot 14.0 program (SPSS Inc., San Jose, CA, USA). After testing for ANOVA assumptions (homogeneity of variances with the Levene's mean test, and normality with the Kolmogorov–Smirnov test), statistical differences among treatments and varieties were evaluated by two-way factorial ANOVA, followed by the post hoc Tukey's test. Afterwards, statistical differences between years (2017 vs. 2018) within each sampling group were evaluated by one-way analysis of variance (ANOVA), followed by the post hoc Tukey's test. For the specific case of chlorophyll *a* fluorescence transient measurements, statistical differences were evaluated by one-way analysis of variance (ANOVA), followed by the post-hoc Tukey's test ( $p < 0.05$ ). Different lower case letters represent significant differences between treatments and varieties (TN\_C, TN\_K, TF\_C, TF\_K) within each region, developmental stage, and growing season. The asterisks (\*  $p < 0.05$ ) represent significant differences between developmental stages (EL35 vs. EL38) within each variety, treatment and sampling year. Absence of letters and asterisks indicate no significant difference.

## 3. Results

### 3.1. Kaolin Effects on *VvHSP70* and *VvWRKY18* Gene Expression

In order to understand kaolin inducing and/or repressive effect on regulating multiple stress responses, we analysed the expression of a heat stress related gene (*VvHSP70*), and a transcription factor related to stress tolerance (*VvWRKY18*) (Figure 2). The relative expression of *VvHSP70* was significantly downregulated in TN kaolin-treated grapevines at stage EL35 in both growing seasons at Alentejo (Figure 2b), whistle in the Douro (Figure 2a) this effect was only noticed in 2017. Conversely, kaolin treatment effects on TF were mostly found in the 2018 growing season, showing approximately an 11-fold *VvHSP70* downregulation compared to the respective control group. Excepting stage EL35 of 2018 in the Douro trial, kaolin effects on *VvWRKY18* gene expression were repressive in TN variety in both regions (Figure 2c,d). In contrast, *VvWRKY18* gene expression in TF treated leaves was upregulated in Alentejo at stage EL38 in both sampling years, while at Douro an opposite trend can be observed during the 2018 growing season.

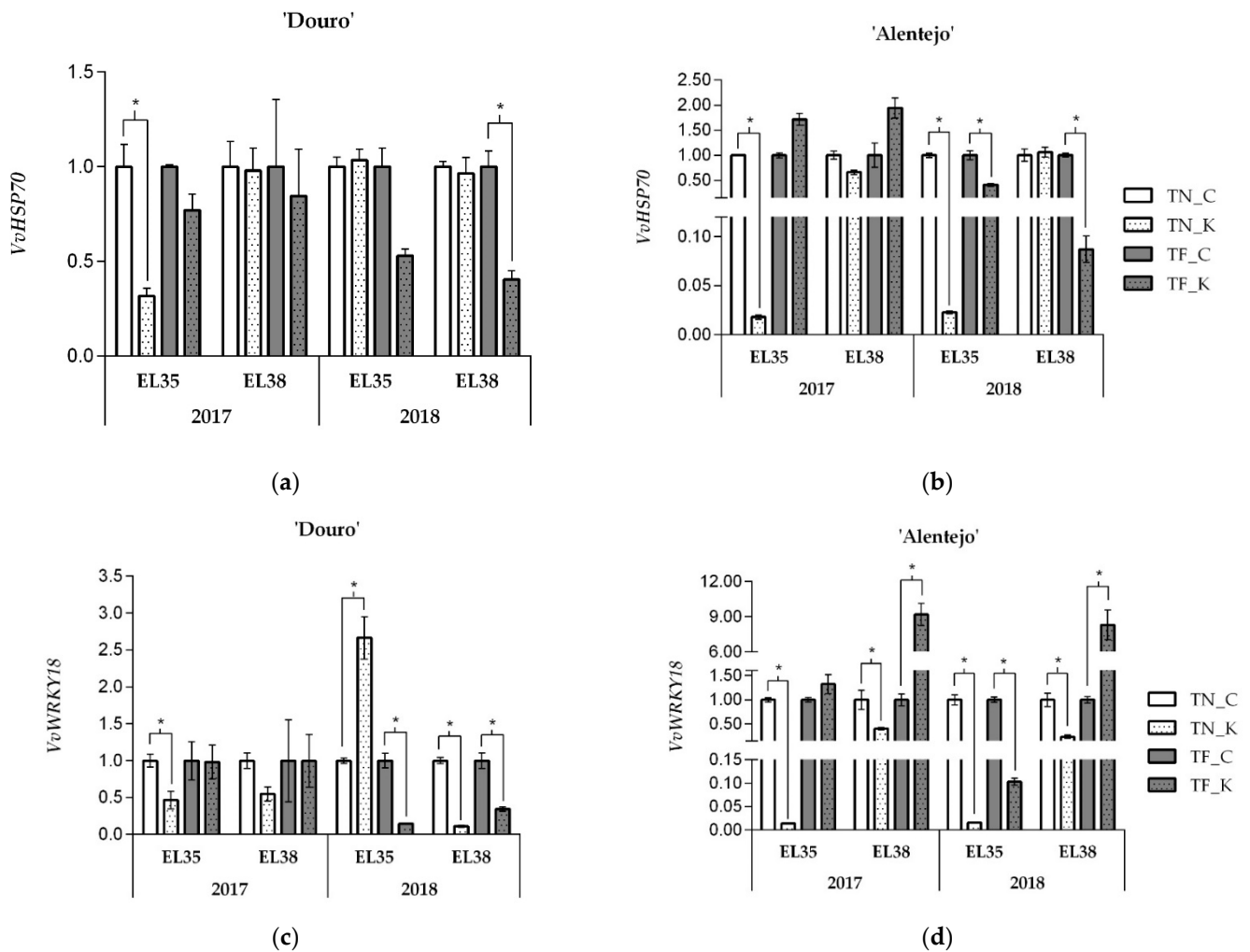


**Figure 2.** Relative expression of *VvHSP70* (a,b), and *VvWRKY18* (c,d) genes of TN and TF grapevine leaves (*Touriga Nacional* control-TN\_C and kaolin-TN\_KL; *Touriga Franca* control-TF\_C and kaolin-TF\_KL) at Douro and Alentejo throughout 2017 and 2018 summer seasons. Values are means of three replications  $\pm$  standard error. \* denote significant difference between control and kaolin treated vines of each variety within the same developmental stage (EL35 or EL38).

### 3.2. Leaf Temperature and Chlorophyll Content

Kaolin effects on leaf cooling and chlorophyll content are shown in Table 2. Though the results do not follow a consistent change throughout the assay in both locations, in the 2017 growing season, TN\_K and TF\_K leaf temperature decreased 11.0% and 4.4%, respectively, at stage EL35 in the Douro trial. At Alentejo, significant kaolin effects on leaf cooling were only found in TF variety at stage EL38 in 2017, and at stage EL35 in the following growing season. Regarding total chlorophyll levels, similar responses can be observed in 2017 in both locations and varieties, with a significant increase in treated leaves throughout the assay, particularly in TF. This response was only found at Douro in the following growing season, whereas TN and TF treated leaves showed 17.5% and 58.8% higher chlorophyll content at stage EL35, respectively.

**Table 2.** Kaolin effects on leaf temperature ( $^{\circ}\text{C}$ ) and total content of chlorophyll ( $\text{mg m}^{-2}$ ) in *Touriga Nacional* and *Touriga Franca* varieties in two developmental stages (EL35 and EL 38), at the Douro and Alentejo trials, during 2017 and 2018 growing seasons.

|                   | Year | Stage | Douro                   |                       |                       |                      | Alentejo                |                       |                       |                       |
|-------------------|------|-------|-------------------------|-----------------------|-----------------------|----------------------|-------------------------|-----------------------|-----------------------|-----------------------|
|                   |      |       | <i>Touriga Nacional</i> |                       | <i>Touriga Franca</i> |                      | <i>Touriga Nacional</i> |                       | <i>Touriga Franca</i> |                       |
|                   |      |       | Control                 | Kaolin                | Control               | Kaolin               | Control                 | Kaolin                | Control               | Kaolin                |
| Leaf Temperature  | 2017 | EL35  | 45.33 $\pm$ 1.78 a      | 40.33 $\pm$ 0.99 c    | 41.78 $\pm$ 1.30 b    | 39.94 $\pm$ 0.92 c   | 31.20 $\pm$ 1.29 ab     | 30.56 $\pm$ 1.17 b    | 33.24 $\pm$ 2.26 a    | 31.94 $\pm$ 1.20 ab   |
|                   |      | EL38  | 37.31 $\pm$ 0.82 b *    | 37.78 $\pm$ 0.70 ab * | 39.35 $\pm$ 1.55 a *  | 38.70 $\pm$ 0.76 ab  | 32.22 $\pm$ 0.93 c      | 32.69 $\pm$ 1.55 cb * | 36.20 $\pm$ 2.18 a *  | 34.72 $\pm$ 1.35 ab * |
|                   | 2018 | EL35  | 31.39 $\pm$ 1.18        | 31.38 $\pm$ 0.80      | 31.17 $\pm$ 1.12      | 30.89 $\pm$ 1.72     | 30.93 $\pm$ 0.91 b      | 30.65 $\pm$ 1.29 b    | 35.89 $\pm$ 1.68 a    | 32.78 $\pm$ 1.36 b    |
|                   |      | EL38  | 37.33 $\pm$ 1.43 *      | 36.61 $\pm$ 1.97 *    | 36.61 $\pm$ 2.07 *    | 35.89 $\pm$ 2.24 *   | 36.50 $\pm$ 1.87 b *    | 35.28 $\pm$ 1.98 b *  | 39.61 $\pm$ 1.93 a *  | 37.06 $\pm$ 1.91 b *  |
| Total Chlorophyll | 2017 | EL35  | 285.3 $\pm$ 20.2 c      | 316.0 $\pm$ 17.8 c    | 386.0 $\pm$ 26.9 b    | 453.2 $\pm$ 21.8 a   | 316.0 $\pm$ 22.7 b      | 431.3 $\pm$ 10.0 a    | 328.0 $\pm$ 32.2 b    | 460.7 $\pm$ 11.2 a    |
|                   |      | EL38  | 353.0 $\pm$ 24.0 b *    | 344.7 $\pm$ 27.4 b    | 380.6 $\pm$ 30.7 b    | 425.5 $\pm$ 34.5 b   | 298.7 $\pm$ 16.5 c      | 393.5 $\pm$ 27.5 a *  | 365.5 $\pm$ 26.3 ab   | 351.8 $\pm$ 27.1 b *  |
|                   | 2018 | EL35  | 333.8 $\pm$ 32.4 c      | 392.2 $\pm$ 24.0 b    | 283.7 $\pm$ 14.3 d    | 450.5 $\pm$ 38.1 a   | 445.0 $\pm$ 26.2        | 438.2 $\pm$ 54.7      | 439.8 $\pm$ 34.0      | 409 $\pm$ 20.4        |
|                   |      | EL38  | 241.3 $\pm$ 23.1 b *    | 247.8 $\pm$ 27.2 b *  | 297.8 $\pm$ 8.0 a     | 309.0 $\pm$ 16.4 a * | 401.0 $\pm$ 24.1 *      | 410.3 $\pm$ 10.7      | 409.0 $\pm$ 48.5      | 406.8 $\pm$ 35.6      |

Data are mean  $\pm$  SD ( $n = 10$ ). Different lower case letters represent significant differences between treatments and varieties within each developmental stage (EL35 and EL38), and sampling year. \* represent significant differences ( $p < 0.05$ ) between developmental stages (EL35 vs. EL38) within each variety, treatment, and sampling year.



### 3.3. Transient Chlorophyll a Fluorescence Analysis by JIP-Test

The relative change of the JIP test parameters in the Douro and Alentejo regions for both growing seasons (Figures 3 and 4), respective to the midday period of each developmental stage (EL35 and EL38), a critical period of extreme atmospheric demand conditions. The phenomenological (ABS/CS) and specific (ABS/RC,  $ET_0/RC$ ,  $DI_0/RC$  and  $TR_0/RC$ ) energy fluxes, quantum efficiencies ( $\phi P_0$ ,  $\Psi_0$  and  $\Psi E_0$ ), and performance index ( $PI_{ABS}$ ) of the Douro trial are shown in Figure 3. At the beginning of the study (Figure 3a), specific energy fluxes show that kaolin treatment resulted in a decrease of the trapping ( $TR_0/RC$ ) and electron transport ( $ET_0/RC$ ) fluxes in both varieties. At the same time, it increased the dissipation energy ( $DI_0/RC$ ) only in TF. Similarly, the absorbed photon flux per cross-section (ABS/CS), which corresponds to the basal fluorescence, and per reaction centre (ABS/RC) were higher in TF treated grapevines, whereas  $PI_{ABS}$  increased exclusively in TN treated vines. On the other hand, the quantum yield and probability of electron transport ( $\Psi_0$  and  $\Psi E_0$ ) increased with kaolin application in TN and decreased in TF. In contrast, the quantum yield of primary photochemistry ( $\phi P_0$ ) was higher in TF treated grapevines, and lower in TN\_K. At EL38 of 2017 growing season (Figure 3b), most of the differences triggered by kaolin application were found in TN, presenting higher quantum efficiencies ( $\phi P_0$ ,  $\Psi_0$ , and  $\Psi E_0$ ),  $PI_{ABS}$ ,  $ET_0/RC$ , and  $DI_0/RC$ . In TF, the positive effects of particle-film application were only noticed on  $PI_{ABS}$  and ABS/CS parameters. In 2018, no significant changes were found for TF at EL35 (Figure 3c), whereas TN\_K showed lower relative values in all specific energy fluxes (ABS/RC,  $TR_0/RC$ ,  $ET_0/RC$ , and  $DI_0/RC$ ), and  $PI_{ABS}$ . At the last stage of the study (Figure 3d), all quantum yield parameters ( $\phi P_0$ ,  $\Psi_0$ , and  $\Psi E_0$ ), as well as the absorption energy per cross-section and the performance index were increased in both treated varieties. Concerning the specific energy fluxes expressed per reaction centre, kaolin positively influenced ABS/RC and  $TR_0/RC$  parameters in TN variety, and  $ET_0/RC$  in TF, at stage EL38.

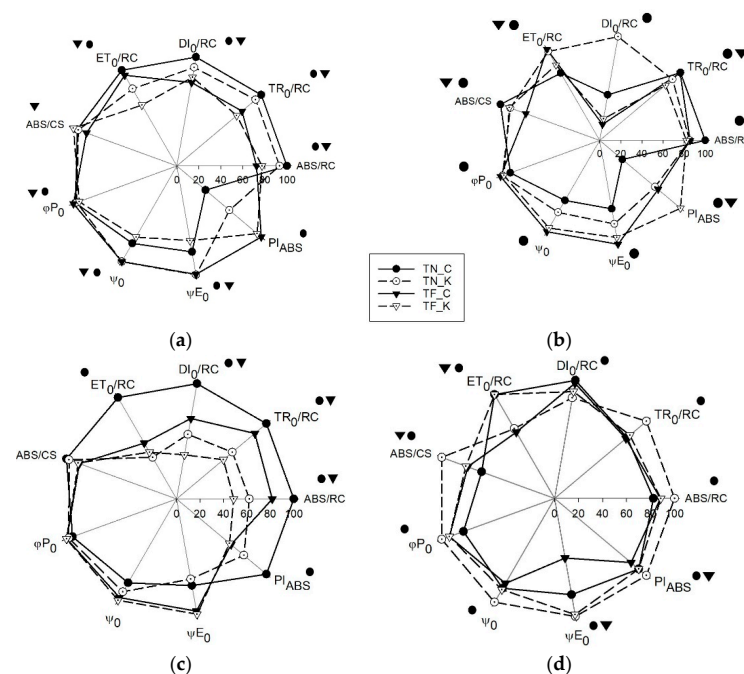


**Figure 3.** Radar plots of JIP parameters deduced from chlorophyll a fluorescence OJIP transients in the grapevine leaves of *Touriga Nacional* control (TN\_C) and kaolin (TN\_K), and *Touriga Franca* control (TF\_C) and kaolin (TF\_K) in the Douro site at stages EL35 and EL38 of 2017 (a,b) and 2018 (c,d). Data are mean  $\pm$  SD ( $n = 18$ ). For each parameter, the lower value represents relative change against the maximum value, set as 100%. Closed circles (●) and triangles (▼) at the top of each parameter represent significant differences between treatments in *Touriga Nacional* and *Touriga Franca*, respectively.

Regarding the Alentejo assay, different tendencies were observed on  $PI_{ABS}$  index at stage EL35 of 2017, in which kaolin had a significant positive effect only in TN (Figure 4a). Additionally, at this stage, TF\_K showed lower quantum efficiencies ( $\phi P_0$ ,  $\Psi_0$ , and  $\Psi E_0$ ), and lower electron transport in an active RC. Throughout the 2017 growing season, kaolin effects on TN and TF photochemistry were weakened in EL38 (Figure 4b), decreasing both the apparent antenna size of an active RC (ABS/RC) and the trapping energy by the RC in TF, without changing the electron transport flux ( $ET_0/RC$ ). Similarly to the results obtained in the previous year, the  $PI_{ABS}$  index was lower in the treated plants of both varieties at stage EL35 of 2018 (Figure 4c). Still, TF\_K showed increased absorption flux per cross-section (ABS/CS), and higher electron transport ( $ET_0/RC$ ) and effective dissipation ( $DI_0/RC$ ) per active RC at this stage. At EL38 of 2018 (Figure 4d),  $PI_{ABS}$  index remained lower in the kaolin treated plants of both varieties, as well as the  $ET_0/RC$  and  $TR_0/RC$  specific fluxes in TF. Oppositely,  $ET_0/RC$ ,  $DI_0/RC$ , and the apparent antenna size (ABS/RC), increased in TN\_K.

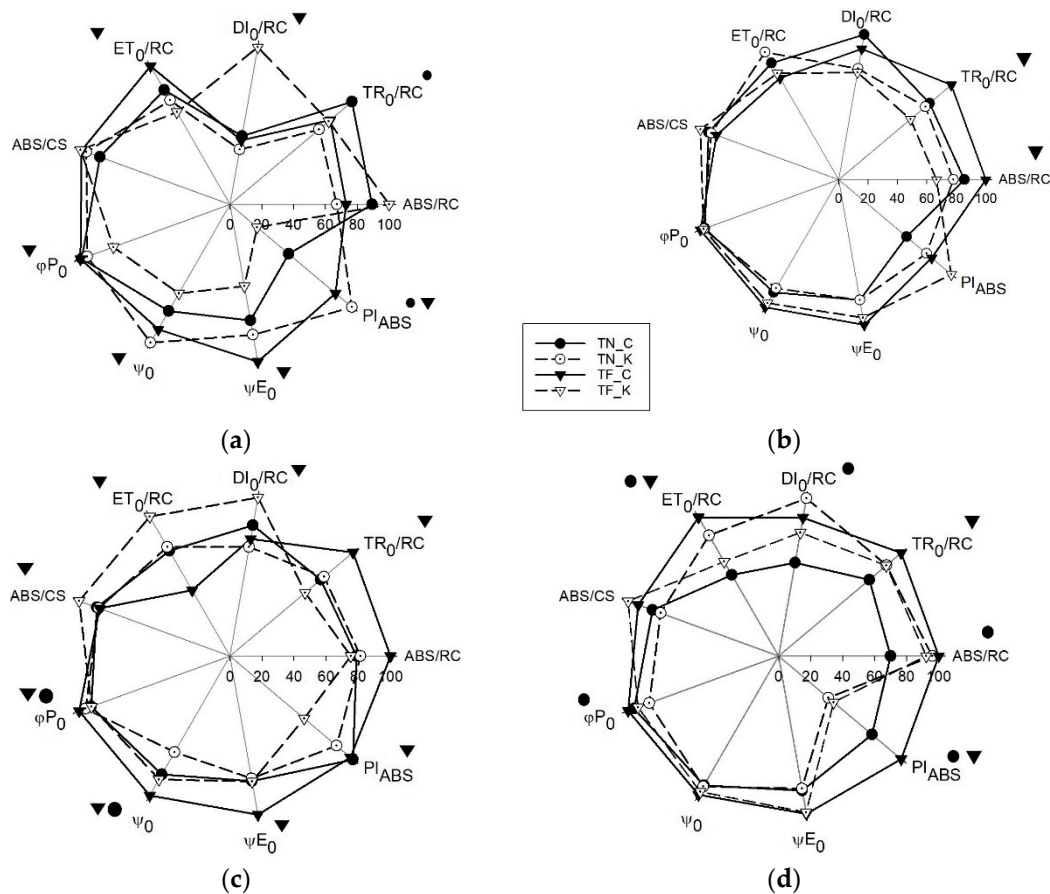


**Figure 4.** Radar plots of JIP parameters deduced from chlorophyll a fluorescence OJIP transients in the grapevine leaves of *Touriga Nacional* control (TN\_C) and kaolin (TN\_K), and *Touriga Franca* control (TF\_C) and kaolin (TF\_K) in the Alentejo site at stages EL35 and EL38 of 2017 (a,b) and 2018 (c,d). Data are mean  $\pm$  SD ( $n = 18$ ). For each parameter, the lower value represents relative change against the maximum value, set as 100%. Closed circles (●) and triangles (▼) at the top of each parameter represent significant differences between treatments in *Touriga Nacional* and *Touriga Franca*, respectively.

### 3.4. Kaolin Effects on Lipid Peroxidation, Proline, and Ascorbate Accumulation

Tables 3 and 4 show different kaolin application responses regarding lipid peroxidation, proline, and ascorbate content depending on the variety. At Douro (Table 3), lipid peroxidation was significantly prevented in TN treated leaves during 2017, while in 2018, this effect was only evident at stage EL35, showing 59.6% less TBARS levels compared to its respective control. In contrast, TF\_K showed higher lipid peroxidation levels at this

stage in both growing seasons, being this effect diluted, and even inverted in 2018, at stage EL38.

**Table 3.** Kaolin effects on the total content of thiobarbituric acid reactive substances (TBARS, mmol MDA<sub>eq</sub> g<sup>-1</sup> DW), proline (μmol g<sup>-1</sup> DW), ascorbate (AsA, mg g<sup>-1</sup> DW), dehydroascorbate (DAsA, mg g<sup>-1</sup> DW), and percentage of ascorbate reduction (%) of *Touriga Nacional* and *Touriga Franca* varieties in two developmental stages (EL35 and EL 38), at the Douro trial, during 2017 and 2018 growing seasons.

| Douro Trial           | Season | Stage | <i>Touriga Nacional</i> |                  | <i>Touriga Franca</i> |                  |
|-----------------------|--------|-------|-------------------------|------------------|-----------------------|------------------|
|                       |        |       | Control                 | Kaolin           | Control               | Kaolin           |
| TBARS                 | 2017   | EL35  | 13.14 ± 1.37 a          | 10.87 ± 2.17 a   | 6.17 ± 1.06 b         | 13.36 ± 0.95 a   |
|                       |        | EL38  | 23.68 ± 2.03 a *        | 15.20 ± 0.27 b * | 1.67 ± 0.26 c *       | 2.07 ± 1.03 c *  |
|                       | 2018   | EL35  | 12.35 ± 2.52 a          | 4.99 ± 1.09 bc   | 2.75 ± 0.56 c         | 6.96 ± 1.62 b    |
|                       |        | EL38  | 9.58 ± 0.72 b *         | 13.18 ± 2.34 a * | 12.62 ± 1.02 a *      | 4.93 ± 0.31 c    |
| Proline               | 2017   | EL35  | 8.20 ± 0.85             | 8.35 ± 0.77      | 7.20 ± 0.57           | 7.53 ± 0.40      |
|                       |        | EL38  | 6.73 ± 0.61 b *         | 6.32 ± 0.56 b *  | 9.85 ± 0.40 a *       | 7.09 ± 0.73 b    |
|                       | 2018   | EL35  | 16.79 ± 1.64 b          | 10.94 ± 0.79 c   | 13.26 ± 0.34 c        | 21.16 ± 2.29 a   |
|                       |        | EL38  | 16.25 ± 1.61 a          | 8.76 ± 0.90 b    | 10.80 ± 0.37 b *      | 15.34 ± 1.42 a * |
| AsA                   | 2017   | EL35  | 2.70 ± 0.16 a           | 1.50 ± 0.10 c    | 0.67 ± 0.07 d         | 1.84 ± 0.08 b    |
|                       |        | EL38  | 2.35 ± 0.25 a *         | 1.59 ± 0.16 b    | 0.73 ± 0.06 c         | 1.54 ± 0.19 b *  |
|                       | 2018   | EL35  | 4.50 ± 0.26 a           | 2.45 ± 0.15 b    | 1.66 ± 0.12 c         | 2.52 ± 0.32 b    |
|                       |        | EL38  | 3.44 ± 0.31 a *         | 3.23 ± 0.21 ab * | 2.87 ± 0.27 a *       | 2.49 ± 0.19 b *  |
| DAsA                  | 2017   | EL35  | 1.23 ± 0.06 c           | 1.43 ± 0.02 b    | 0.34 ± 0.01 d         | 1.64 ± 0.06 a    |
|                       |        | EL38  | 1.58 ± 0.14 a *         | 0.20 ± 0.02 d *  | 0.56 ± 0.05 c *       | 0.89 ± 0.08 b *  |
|                       | 2018   | EL35  | 1.90 ± 0.30 ab          | 1.77 ± 0.05 ab   | 1.61 ± 0.16 b         | 1.92 ± 0.18 a    |
|                       |        | EL38  | 1.49 ± 0.17 bc *        | 2.57 ± 0.12 a *  | 1.77 ± 0.11 b         | 1.21 ± 0.04 c *  |
| % reduction ascorbate | 2017   | EL35  | 81.65 ± 3.72 a          | 31.15 ± 0.73 c   | 52.53 ± 2.42 b        | 12.88 ± 1.76 d   |
|                       |        | EL38  | 78.73 ± 1.93 b          | 89.28 ± 3.24 a * | 33.25 ± 1.65 d *      | 59.66 ± 8.88 c * |
|                       | 2018   | EL35  | 49.81 ± 2.53 a          | 30.68 ± 2.73 b   | 42.52 ± 5.95 a        | 24.05 ± 1.97 b   |
|                       |        | EL38  | 53.80 ± 2.21 b          | 67.51 ± 4.90 a * | 27.17 ± 4.96 c *      | 55.52 ± 2.40 b * |

Data are mean ± SD ( $n = 6$ ). Different lower case letters represent significant differences between treatments and varieties within each developmental stage (EL35 and EL38), and sampling year. The asterisks (\*) indicate significant differences ( $p < 0.05$ ) between developmental stages (EL35 vs. EL38) within each variety, treatment, and sampling year.

At Alentejo (Table 4), analyses from 2017 to 2018 growing seasons showed a similar pattern in kaolin coated leaves of both varieties, though lipid peroxidation levels were generally higher at the Alentejo trial in all sampling dates regardless the treatment. Regarding proline content, no significant effects were detected in 2017. In 2018, despite presenting an opposite varietal effect, similar responses to kaolin treatment were detected in both regions within each variety, particularly at stage EL38. At this stage, TN treated leaves from Douro and Alentejo showed 46.1% and 7.3% lower proline content, respectively, while TF\_K showed an increase of 42.0% and 75.3%, respectively. Kaolin coating effects on AsA and DAsA were mostly observed at the Douro trial (Table 3) with an opposite trend between varieties. While TN treated leaves showed lower AsA accumulation throughout the season, TF\_K showed higher AsA content, excepting at stage EL38 of the 2018 growing season. Nevertheless, kaolin effect on ascorbate reduction was identical in both varieties and growing seasons at Douro, with significant lower percentage reduction at the stages EL35, and higher at EL38.

**Table 4.** Kaolin effects on the total content of thiobarbituric acid reactive substances (TBARS, mmol MDA<sub>eq</sub> g<sup>-1</sup> dry weight (DW)), proline (μmol g<sup>-1</sup> DW), ascorbate (AsA, mg g<sup>-1</sup> DW), dehydroascorbate (DAsA, mg g<sup>-1</sup> DW), and percentage of ascorbate reduction (%) of *Touriga Nacional* and *Touriga Franca* varieties in two developmental stages (EL35 and EL 38), at the Alentejo trial, during 2017 and 2018 growing seasons.

| Alentejo Trial        | Season | Stage | <i>Touriga Nacional</i> |                   | <i>Touriga Franca</i> |                  |
|-----------------------|--------|-------|-------------------------|-------------------|-----------------------|------------------|
|                       |        |       | Control                 | Kaolin            | Control               | Kaolin           |
| TBARS                 | 2017   | EL35  | 43.11 ± 2.09 a          | 28.52 ± 3.30 b    | 13.17 ± 1.82 d        | 21.85 ± 1.66 c   |
|                       |        | EL38  | 18.17 ± 0.84 a *        | 14.41 ± 1.03 ab * | 13.61 ± 0.45 b        | 13.48 ± 1.29 b * |
|                       | 2018   | EL35  | 30.86 ± 4.27 a          | 20.94 ± 2.52 b    | 12.41 ± 0.88 c        | 6.80 ± 0.42 d    |
|                       |        | EL38  | 20.30 ± 3.17 a *        | 11.07 ± 3.08 b *  | 11.36 ± 1.72 b        | 10.00 ± 2.48 b   |
| Proline               | 2017   | EL35  | 4.73 ± 0.50 b           | 4.29 ± 0.08 b     | 7.47 ± 0.82 a         | 7.84 ± 0.52 a    |
|                       |        | EL38  | 6.86 ± 0.51 b *         | 8.13 ± 0.66 a *   | 7.51 ± 0.50 ab        | 8.00 ± 0.85 ab   |
|                       | 2018   | EL35  | 8.65 ± 1.08 b           | 8.46 ± 0.79 b     | 12.04 ± 0.88 a        | 13.65 ± 0.86 a   |
|                       |        | EL38  | 11.10 ± 0.27 a *        | 10.29 ± 0.47 a *  | 9.86 ± 0.85 a *       | 17.28 ± 2.23 b * |
| AsA                   | 2017   | EL35  | 4.65 ± 0.40 a           | 2.45 ± 0.27 b     | 1.21 ± 0.07 d         | 1.47 ± 0.15 c    |
|                       |        | EL38  | 1.41 ± 0.06 a *         | 1.39 ± 0.12 a *   | 0.65 ± 0.03 b *       | 0.54 ± 0.05 b *  |
|                       | 2018   | EL35  | 3.82 ± 0.40 b           | 4.98 ± 0.55 a     | 2.55 ± 0.18 c         | 3.03 ± 0.14 c    |
|                       |        | EL38  | 3.64 ± 0.38 b           | 4.16 ± 0.34 a *   | 1.51 ± 0.12 d *       | 2.46 ± 0.14 c *  |
| DAsA                  | 2017   | EL35  | 2.22 ± 0.26 a           | 1.10 ± 0.08 b     | 0.65 ± 0.07 c         | 0.69 ± 0.04 c    |
|                       |        | EL38  | 0.70 ± 0.09 a *         | 0.75 ± 0.04 a *   | 0.27 ± 0.02 b *       | 0.18 ± 0.02 b *  |
|                       | 2018   | EL35  | 1.29 ± 0.07 c           | 1.46 ± 0.15 c     | 2.66 ± 0.21 a         | 1.91 ± 0.25 b    |
|                       |        | EL38  | 1.98 ± 0.18 a *         | 1.32 ± 0.12 b     | 1.42 ± 0.07 b *       | 1.42 ± 0.20 b *  |
| % reduction ascorbate | 2017   | EL35  | 58.05 ± 4.63 b          | 59.58 ± 4.14 b    | 71.63 ± 6.60 a        | 60.42 ± 1.79 b   |
|                       |        | EL38  | 70.38 ± 4.05 b *        | 71.32 ± 5.96 b *  | 59.31 ± 1.78 c *      | 92.17 ± 8.90 a * |
|                       | 2018   | EL35  | 70.14 ± 3.14 a          | 70.38 ± 3.04 a    | 7.08 ± 1.66 c         | 28.15 ± 3.52 b   |
|                       |        | EL38  | 44.12 ± 1.30 b *        | 69.14 ± 2.64 a    | 29.08 ± 6.13 c *      | 68.45 ± 1.78 a * |

Data are mean ± SD ( $n = 6$ ). Different lower case letters represent significant differences between treatments and varieties within each developmental stage (EL35 and EL38), and sampling year. The asterisks (\*) indicate significant differences ( $p < 0.05$ ) between developmental stages (EL35 vs. EL38) within each variety, treatment, and sampling year.

#### 4. Discussion

The combined hot and dry local conditions (Table 1 and Figure 1) can lead to frequent and persistent damages at physiological, biochemical, and molecular levels, highlighting the critical role of using mitigation practices in alleviating summer stress impacts [29,30].

Overall, the downregulation of *VvHSP70* gene expression in treated leaves (Figure 2), particularly at the Alentejo site, reinforces the kaolin protective role against summer stress, considering that most HSP groups are generally upregulated under stressful conditions [31]. In agreement, a similar effect was observed upon stress exposure and recovery of ‘Cabernet Sauvignon’ leaves, demonstrating that most HSP genes were upregulated by heat stress, but not during recovery, supporting the hypothesis particle film technology may alleviate heat stress factors on grapevines. Likewise, *VvWRKY18* gene expression was mainly downregulated in treated grapevines from TN in both regions and upregulated in TF at the Alentejo trial, indicating different varietal responses to kaolin application that could depend on other factors, such as rootstock, *terroir*, and stress severity [3,5,32]. It is also plausible that these differences might be related to intrinsic varietal features, such as the phenological onset of the *veraison* stage and leaf senescence mechanisms [31,33]. One of the major impacts of climate change in temperate climate regions is the earlier onset of several phenological stages associated with variations in the maximum temperature and varietal heat requirements [34,35]. Indeed, in a comparative study on grapevine phenology performed in the same varieties of this work, Costa et al. [33] reported an earlier *veraison* timing for TF respecting TN in most climatic models applied, supporting the varietal differences found in *VvHSP70* and *VvWRKY18* gene expression in the current conditions. Nevertheless, these findings suggest that the use of particle film technology lowers the need for triggering heat stress tolerance mechanisms, and related gene expression of grapevines grown in Mediterranean-type climate vineyards.

Kaolin leaf cooling effects differed among regions (Table 2), with lower leaf temperature mostly found at stage EL35 at Douro, suggesting that regional edaphoclimatic conditions could be the paramount factor in shaping plant stress responses. Leaf cooling effect by reflective particle films application was extensively reported in previous studies in grapevines [10,11,13] and other crops [36,37]. However, it is also worth stating that the extent of this effect may be varietal dependent and affected by the leaf water status [32]. Besides, the present effect of kaolin on promoting chlorophyll accumulation under stressful conditions, and thus preventing photo-oxidative damage, supports evidence from previous research on several crops, such as grapevines [14,38], wheat [39] and olive [29], and apple [40] trees.

Regarding chlorophyll *a* fluorescence transient analysis, the specific energy flux data, combined with the quantum yield analysis, highlight different varietal responses in both regions (Figures 3 and 4), particularly in 2017 at the *veraison* stage (EL35). At this stage, specific energy fluxes ( $TR_0/RC$  and  $ET_0/RC$ ), yield of primary photochemistry ( $\phi P_0$ ), and  $ABS/RC$  decreased in TN\_K, indicating an apparent antenna size reduction and lower inactivation of RC's at the beginning of the experiment, which might explain the higher performance index ( $PI_{ABS}$ ) found in TN\_K at both sites, as previously observed by Dinis et al. [38]. Interestingly, TF seems to have adopted a slightly different light absorption strategy, showing decreased  $TR_0/RC$  and  $ET_0/RC$ , lower  $\Psi_0$ , and  $\Psi E_0$ , but increased  $\phi P_0$ ,  $ABS/RC$ , and  $DI_0/RC$  in kaolin treated grapevines, with no influence on the  $PI_{ABS}$  index. These results suggest a safe downregulation mechanism, which includes a decrease of the fraction of fully active RC, and increase of the heat sink centres to dissipate excess energy, as pointed on the findings of Beneragama et al. [41]. Nonetheless, this downregulation can also be related to non-quinone A ( $Q_A$ ) reducing RC, known as silent RC [42]. The positive effects of kaolin on grapevine performance ( $PI_{ABS}$ ) increased at ripening (EL38), in both varieties from the Douro site (Figure 3), but not in Alentejo (Figure 4), indicating that particle film efficiency on promoting plant stress responses might be different from site-to-site, depending on stress severity and extent, as well as on the initial foliar acclimation mechanisms to kaolin treatment. In agreement, results from 2018 show no significant influence of particle film application on chlorophyll transient analysis, particularly at the Alentejo, whereas at Douro, treated grapevines continued exhibiting higher  $PI_{ABS}$ , suggesting increased kaolin effectiveness under severe environmental conditions. Since 2017 was warmer and drier than 2018, with the occurrence of two heatwave events and low rainfall levels, it seems likely that stress severity and impacts were more pronounced in the 2017 growing season, which can modulate kaolin efficiency in alleviating summer stress.

The levels of reduced and oxidised ascorbate, as well as the percentage reduction, indicated that TF and TN have different basal levels of ascorbate, and that kaolin promoted different responses to ascorbate accumulation. Overall, kaolin foliar treatment promoted the accumulation of reduced and oxidised ascorbate only at Douro (Table 3), indicating some predisposition to react under stressful conditions [5]. Despite the general reducing effect on the lipid peroxidation levels observed in both treated varieties within each region, which reinforces the protective role of kaolin, the findings of the current study do not clearly support the tendency for lowering proline accumulation in kaolin treated grapevines exposed to summer stress [43,44]. In fact, at Alentejo, proline levels were mainly higher in TF treated vines, indicating a lower need for kaolin application on this variety at the beginning of ripening. Even so, kaolin application under milder stress conditions, such as those recorded in 2018 that were characterised by the occurrence of only one heatwave event and higher rainfall levels compared to 2017, could also induce positive feedback on plant stress responses by increasing the accumulation of metabolites responsible for cellular homeostasis. Moreover, it should also bear in mind that plant response to multiple factors can be unique and differ from a single stress factors [9,45]. Under field conditions, these observations suggest that some stress factors prevail among others, changing the accumulation of several foliar stress-related metabolites.

## 5. Conclusions

In summary, the assessment of kaolin particle film efficiency in climate change hotspot regions through multiple-based approaches (physiological, biochemical, and molecular) revealed regulation of heat stress responses and tolerance mechanisms, and improved summer stress responses and photochemistry modulation under stress conditions. The results indicate different varietal responses to kaolin application in each region, while highlighting the viticultural environment as the paramount factor in shaping grapevine stress responses. Moreover, this research allows studying plant stress responses and acclimation mechanisms pragmatically and reveals the complexity of studying adult plants in commercial vineyards. From a climate change perspective, comparative studies should be further explored under controlled and field conditions to elucidate the advantages of particle film application on other Mediterranean crops' production and quality.

**Author Contributions:** Conceptualization, A.C.M., C.C., J.M.-P. and L.-T.D.; data curation, S.B., V.V.-P., J.M.-P. and L.-T.D.; formal analysis, S.B. and V.V.-P.; funding acquisition, A.C.M., C.C., J.M.-P. and L.-T.D.; investigation, S.B., A.L., N.M., H.F., V.V.-P., J.M.-P. and L.-T.D.; methodology, S.B., J.M.-P. and L.-T.D.; project administration, C.C. and J.M.-P.; resources, V.V.-P., A.G.-C. and J.M.-P.; supervision, N.M., J.M.-P. and L.-T.D.; validation, S.B., A.L. and V.V.-P.; visualization, S.B., J.M.-P. and L.-T.D.; writing—original draft, S.B.; writing—review and editing, A.L., N.M., V.V.-P., A.C.M., C.C., A.G.-C., J.M.-P. and L.-T.D. All authors have read and agreed to the published version of the manuscript.

**Funding:** This research was funded with national funds from the FCT-Portuguese Foundation for Science and Technology, under project UIDB/04033/2020, the Clim4Vitis project—“Climate change impact mitigation for European viticulture: knowledge transfer for an integrated approach”, funded by European Union's Horizon 2020 research and innovation programme, under grant agreement no. 810176, and by project I&D&I AgriFood XXI, operation NORTE-01-0145-FEDER-000041, co-funded by European Regional Development Fund (FEDER) through NORTE 2020 (Programa Operacional Regional do Norte 2014/2020). Sara Bernardo acknowledges the financial support provided by the FCT-Portuguese Foundation for Science and Technology (PD/BD/128273/2017), under the Doctoral Programme “Agricultural Production Chains—from fork to farm”. Ana Luzio thanks the postdoctoral fellowship (BPD/INTERACT/VITALITYWINE/184/2016) and Dinis, L.-T. thanks the FCT and UTAD for the research contract (D.L. Law no. 57/2017).

**Institutional Review Board Statement:** Not applicable.

**Informed Consent Statement:** Not applicable.

**Data Availability Statement:** The data presented in this study are available on request from the corresponding author.

**Acknowledgments:** Authors acknowledge Rui Flores from “Herdade do Esporão” and Daniel Gomes from “Quinta do Orgal, Vallado”, for the collaboration and efforts in making the vineyard facilities available for this study, as well as the BASF collaboration, namely Paulo Matos.

**Conflicts of Interest:** The authors declare no conflict of interest. The funders had no role in the design of the study; in the collection, analyses, or interpretation of data; in the writing of the manuscript, or in the decision to publish the results.

## Appendix A

**Table A1.** List of Primers Used for Real-Time Quantitative PCR.

| Gene            | Gene Unique ID    |          | Primer (5'–3')                                | Size (bp) |
|-----------------|-------------------|----------|---|-----------|
| <i>VvHSP70</i>  | GSVIVT01008331001 | Fw<br>Rv | GACCTTGGGGGTGGTACTTT<br>GCCAACCAATCCACAACCTCT | 131       |
| <i>VvWRKY18</i> | GSVIVT01035885001 | Fw<br>Rv | GAAGCCAAGAGAAAGCACCA<br>GGCTCTGGGAGAAGGGTTAT  | 145       |
| <i>VvACT2</i>   | GSVIVT01026580001 | Fw<br>Rv | GCCATCCAAGCTGTTCTCTC<br>CAGTAAGGTCACGTCCAGCA  | 157       |
| <i>VvTUB2</i>   | GSVIVT01037405001 | Fw<br>Rv | CAACTCTGACCTCCGAAAGC<br>CTGGAGTCCCACATTGCT    | 154       |

## References

1. Giorgi, F. Climate change hot-spots. *Geophys. Res. Lett.* **2006**, *33*. [\[CrossRef\]](#)
2. Santos, J.A.; Fraga, H.; Malheiro, A.C.; Moutinho-Pereira, J.; Dinis, L.-T.; Correia, C.; Moriondo, M.; Leolini, L.; Dibari, C.; Costafreda-Aumedes, S.; et al. A review of the potential climate change impacts and adaptation options for European viticulture. *Appl. Sci.* **2020**, *10*, 3092. [\[CrossRef\]](#)
3. Bernardo, S.; Dinis, L.-T.; Machado, N.; Moutinho-Pereira, J. Grapevine abiotic stress assessment and search for sustainable adaptation strategies in Mediterranean-like climates. A review. *Agron. Sustain. Dev.* **2018**, *38*. [\[CrossRef\]](#)
4. Zandalinas, S.I.; Mittler, R.; Balfagón, D.; Arbona, V.; Gómez-Cadenas, A. Plant adaptations to the combination of drought and high temperatures. *Physiol. Plant.* **2018**, *162*, 2–12. [\[CrossRef\]](#)
5. Carvalho, L.C.; Coito, J.L.; Colaço, S.; Sangiogo, M.; Amâncio, S. Heat stress in grapevine: The pros and cons of acclimation. *Plant Cell Environ.* **2015**, *38*, 777–789. [\[CrossRef\]](#)
6. Vives-Peris, V.; Marmaneu, D.; Gomez-Cadenas, A.; Perez-Clemente, R.M. Characterization of Citrus WRKY transcription factors and their responses to phytohormones and abiotic stresses. *Biol. Plant.* **2018**, *62*, 33–44. [\[CrossRef\]](#)
7. Akram, N.A.; Shafiq, F.; Ashraf, M. Ascorbic Acid-A Potential Oxidant Scavenger and Its Role in Plant Development and Abiotic Stress Tolerance. *Front. Plant Sci.* **2017**, *8*, 613. [\[CrossRef\]](#)
8. Masouleh, S.S.S.; Aldine, N.J.; Sassine, Y.N. The role of organic solutes in the osmotic adjustment of chilling-stressed plants (vegetable, ornamental and crop plants). *Ornam. Hortic.* **2019**, *25*, 434–442. [\[CrossRef\]](#)
9. Mittler, R. Abiotic stress, the field environment and stress combination. *Trends Plant Sci.* **2006**, *11*, 15–19. [\[CrossRef\]](#)
10. Brillante, L.; Belfiore, N.; Gaiotti, F.; Lovat, L.; Sansone, L.; Poni, S.; Tomasi, D. Comparing kaolin and pinolene to improve sustainable grapevine production during drought. *PLoS ONE* **2016**, *11*, e0156631. [\[CrossRef\]](#) [\[PubMed\]](#)
11. Dinis, L.T.; Malheiro, A.C.; Luzio, A.; Fraga, H.; Ferreira, H.; Goncalves, I.; Pinto, G.; Correia, C.M.; Moutinho-Pereira, J. Improvement of grapevine physiology and yield under summer stress by kaolin-foliar application: Water relations, photosynthesis and oxidative damage. *Photosynthetica* **2018**, *56*, 641–651. [\[CrossRef\]](#)
12. Frioni, T.; Tombesi, S.; Sabbatini, P.; Squeri, C.; Lavado Rodas, N.; Palliotti, A.; Poni, S. Kaolin reduces ABA biosynthesis through the inhibition of neoxanthin synthesis in grapevines under water deficit. *Int. J. Mol. Sci.* **2020**, *21*, 4950. [\[CrossRef\]](#)
13. Glenn, D.M.; Cooley, N.; Walker, R.; Clingeffer, P.; Shellie, K. Impact of kaolin particle film and water deficit on wine grape water use efficiency and plant water relations. *HortScience* **2010**, *45*, 1178–1187. [\[CrossRef\]](#)
14. Shellie, K.C.; King, B.A. Kaolin particle film and water deficit influence Malbec leaf and berry temperature, pigments, and photosynthesis. *Am. J. Enol. Vitic.* **2013**, *64*, 223–230. [\[CrossRef\]](#)
15. FAO. *International Soil Classification System for Naming Soils and Creating Legends for Soil Maps*; World Soil Resources Reports; IUSS Working Group WRB, World Reference Base for Soil Resources: Rome, Italy, 2015.
16. Coombe, B.G. Growth stages of the grapevine: Adoption of a system for identifying grapevine growth stages. *Aust. J. Grape Wine Res.* **1995**, *1*, 104–110. [\[CrossRef\]](#)
17. Kottek, M.; Grieser, J.; Beck, C.; Rudolf, B.; Rubel, F. World map of the Köppen-Geiger climate classification updated. *Meteorol. Z.* **2006**, *15*, 259–263. [\[CrossRef\]](#)
18. Tonietto, J.; Carbonneau, A. A multicriteria climatic classification system for grape-growing regions worldwide. *Agric. For. Meteorol.* **2004**, *124*, 81–97. [\[CrossRef\]](#)
19. Fraga, H.; Molitor, D.; Leolini, L.; Santos, J.A. What Is the Impact of Heatwaves on European Viticulture? A Modelling Assessment. *Appl. Sci.* **2020**, *10*, 3030. [\[CrossRef\]](#)
20. Gambino, G.; Perrone, I.; Gribaudo, I. A rapid and effective method for RNA extraction from different tissues of grapevine and other woody plants. *Phytochem. Anal.* **2008**, *19*, 520–525. [\[CrossRef\]](#)
21. Pfaffl, M.W. A new mathematical model for relative quantification in real-time RT-PCR. *Nucleic Acids Res.* **2001**, *29*, e45. [\[CrossRef\]](#)
22. Pfaffl, M.W. Relative expression software tool (REST(C)) for group-wise comparison and statistical analysis of relative expression results in real-time PCR. *Nucleic Acids Res.* **2002**, *30*, e36. [\[CrossRef\]](#)
23. Hodges, D.M.; DeLong, J.M.; Forney, C.F.; Prange, R.K. Improving the thiobarbituric acid-reactive-substances assay for estimating lipid peroxidation in plant tissues containing anthocyanin and other interfering compounds. *Planta* **1999**, *207*, 604–611. [\[CrossRef\]](#)
24. Bates, L.S.; Waldren, R.P.; Teare, I.D. Rapid determination of free proline for water-stress studies. *Plant Soil* **1973**, *39*, 205–207. [\[CrossRef\]](#)
25. Okamura, M. An improved method for determination of l-ascorbic acid and l-dehydroascorbic acid in blood plasma. *Clin. Chim. Acta* **1980**, *103*, 259–268. [\[CrossRef\]](#) [\[PubMed\]](#)
26. Strasser, B.J.; Strasser, R.J. Measuring Fast Fluorescence Transients to Address Environmental Questions: The JIP-Test. In *Photosynthesis: From Light to Biosphere*; KAP Press: Dordrecht, The Netherlands, 1995; pp. 4869–4872. [\[CrossRef\]](#)
27. Strasser, R.J.; Srivastava, A.; Tsimilli-Michael, M. The fluorescence transient as a tool to characterize and screen photosynthetic samples. In *Probing Photosynthesis: Mechanisms, Regulation and Adaptation*; Yunus, M., Pathre, U., Mohanty, P., Eds.; Taylor & Francis Publishers: London, UK, 2000; pp. 445–483.
28. Strasser, R.J.; Tsimilli-Michael, M.; Srivastava, A. Analysis of the Chlorophyll a Fluorescence Transient. In *Chlorophyll a Fluorescence*; Springer: Dordrecht, The Netherlands, 2004; Volume 19, pp. 321–362. [\[CrossRef\]](#)

29. Brito, C.; Dinis, L.-T.; Ferreira, H.; Rocha, L.; Pavia, I.; Moutinho-Pereira, J.; Correia, C.M. Kaolin particle film modulates morphological, physiological and biochemical olive tree responses to drought and rewatering. *Plant Physiol. Biochem.* **2018**, *133*, 29–39. [[CrossRef](#)] [[PubMed](#)]
30. Conde, A.; Neves, A.; Breia, R.; Pimentel, D.; Dinis, L.-T.; Bernardo, S.; Correia, C.M.; Cunha, A.; Gerós, H.; Moutinho-Pereira, J. Kaolin particle film application stimulates photoassimilate synthesis and modifies the primary metabolome of grape leaves. *J. Plant Physiol.* **2018**, *223*, 47–56. [[CrossRef](#)] [[PubMed](#)]
31. Kobayashi, M.; Katoh, H.; Takayanagi, T.; Suzuki, S. Characterization of thermotolerance-related genes in grapevine (*Vitis vinifera*). *J. Plant Physiol.* **2010**, *167*, 812–819. [[CrossRef](#)] [[PubMed](#)]
32. Frioni, T.; Saracino, S.; Squeri, C.; Tombesi, S.; Palliotti, A.; Sabbatini, P.; Magnanini, E.; Poni, S. Understanding kaolin effects on grapevine leaf and whole-canopy physiology during water stress and re-watering. *J. Plant Physiol.* **2019**, *242*, 153020. [[CrossRef](#)] [[PubMed](#)]
33. Costa, R.; Fraga, H.; Fonseca, A.; García de Cortázar-Atauri, I.; Val, M.C.; Carlos, C.; Reis, S.; Santos, J.A. Grapevine phenology of cv. Touriga Franca and Touriga Nacional in the Douro wine region: Modelling and climate change projections. *Agronomy* **2019**, *9*, 210. [[CrossRef](#)]
34. García de Cortázar-Atauri, I.; Duchêne, E.; Destrac-Irvine, A.; Barbeau, G.; De Rességuier, L.; Lacombe, T.; Parker, A.K.; Saurin, N.; Van Leeuwen, C. Grapevine phenology in France: From past observations to future evolutions in the context of climate change. *OENO One* **2017**, *51*, 115–126. [[CrossRef](#)]
35. Reis, S.; Fraga, H.; Carlos, C.; Silvestre, J.; Eiras-Dias, J.; Rodrigues, P.; Santos, J.A. Grapevine Phenology in Four Portuguese Wine Regions: Modeling and Predictions. *Appl. Sci.* **2020**, *10*, 3708. [[CrossRef](#)]
36. Abou-Khaled, A.; Hagan, R.M.; Davenport, D.C. Effects of kaolin as a reflective antitranspirant on leaf temperature, transpiration, photosynthesis, and water-use efficiency. *Water Resour. Res.* **1970**, *6*, 280–289. [[CrossRef](#)]
37. Brito, C.; Dinis, L.-T.; Moutinho-Pereira, J.; Correia, C. Kaolin, an emerging tool to alleviate the effects of abiotic stresses on crop performance. *Sci. Hortic.* **2019**, *250*, 310–316. [[CrossRef](#)]
38. Dinis, L.T.; Ferreira, H.; Pinto, G.; Bernardo, S.; Correia, C.M.; Moutinho-Pereira, J. Kaolin-based, foliar reflective film protects photosystem II structure and function in grapevine leaves exposed to heat and high solar radiation. *Photosynthetica* **2016**, *54*, 47–55. [[CrossRef](#)]
39. Abdallah, M.M.S.; El-Bassiouny, H.M.S.; AbouSeeda, M.A. Potential role of kaolin or potassium sulfate as anti-transpirant on improving physiological, biochemical aspects and yield of wheat plants under different watering regimes. *Bull. Natl. Res. Cent.* **2019**, *43*. [[CrossRef](#)]
40. Faghhi, S.; Zamani, Z.; Fatahi, R.; Liaghat, A. Effects of deficit irrigation and kaolin application on vegetative growth and fruit traits of two early ripening apple cultivars. *Biol. Res.* **2019**, *52*. [[CrossRef](#)] [[PubMed](#)]
41. Beneragama, C.K.; Balasooriya, B.L.H.N.; Perera, T.M.R.S. Use of O-J-I-P chlorophyll fluorescence transients to probe multiple effects of UV-C radiation on the photosynthetic apparatus of *Euglena*. *Int. J. Appl. Sci. Biotechnol.* **2014**, *2*, 553–558. [[CrossRef](#)]
42. Strasser, B.J. Donor side capacity of Photosystem II probed by chlorophyll a fluorescence transients. *Photosyn. Res.* **1997**, *52*, 147–155. [[CrossRef](#)]
43. Bernardo, S.; Dinis, L.T.; Luzio, A.; Pinto, G.; Meijón, M.; Valledor, L.; Conde, A.; Gerós, H.; Correia, C.M.; Moutinho-Pereira, J. Kaolin particle film application lowers oxidative damage and DNA methylation on grapevine (*Vitis vinifera* L.). *Environ. Exp. Bot.* **2017**, *139*, 39–47. [[CrossRef](#)]
44. Dinis, L.T.; Bernardo, S.; Luzio, A.; Pinto, G.; Meijón, M.; Pintó-Marijuan, M.; Cotado, A.; Correia, C.; Moutinho-Pereira, J. Kaolin modulates ABA and IAA dynamics and physiology of grapevine under Mediterranean summer stress. *J. Plant Physiol.* **2018**, *220*, 181–192. [[CrossRef](#)] [[PubMed](#)]
45. Rizhsky, L.; Liang, H.; Shuman, J.; Shulaev, V.; Davletova, S.; Mittler, R. When Defense Pathways Collide. The Response of Arabidopsis to a Combination of Drought and Heat Stress. *Plant Physiol.* **2004**, *134*, 1683–1696. [[CrossRef](#)] [[PubMed](#)]